doi:10.1246/cl.2011.1395
Published on the web November 26, 2011

A Nonadiabatic Ab Initio Dynamics Study on Rhodopsin and Its Analog Isorhodopsin: Chemical Dynamics Reasons behind Selection of Rhodopsin by Life

Wilfredo Credo Chung,*[1] Shinkoh Nanbu,[2] and Toshimasa Ishida[1]
[1]*Fukui Institute for Fundamental Chemistry, Kyoto University, 34-4 Takano-nishihirakicho, Sakyo-ku, Kyoto 606-8103*
[2]*Department of Materials and Life Sciences, Faculty of Science and Engineering, Sophia University, Kioicho, Chiyoda-ku, Tokyo 102-8554*

(Received August 31, 2011; CL-110725; E-mail: wchung@fukui.kyoto-u.ac.jp)

The structural difference between rhodopsin and isorhodopsin is only in the *cis*-position of the chromophore, but the difference leads to a large discrepancy in photoisomerization period and quantum yield. The photoinduced *cis–trans* isomerization dynamics of the two chromophores are investigated using a Quantum Mechanics/Molecular Mechanics trajectory surface hopping scheme. Rhodopsin shows a straightforward and fast excited-state dynamics whereas the isorhodopsin dynamics in the excited state is complicated due to differences in retinal motions and space gaps formed by surrounding residues. Consequently, the isorhodopsin → bathorhodopsin reaction is slower and less efficient. Photoexcitation of rhodopsin gives bathorhodopsin only, whereas isorhodopsin yields an analog with 9,11-di-*cis*-retinal in addition to bathorhodopsin. These differences explain why life uses rhodopsin rather than isorhodopsin.

Rhodopsin (Rh) has 11-*cis*-retinal as chromophore and is the photosensitive chemical found on the outer segment of rod-like cells in the retina, the light-sensing structure of the eye.[1] Isorhodopsin (isoRh) is an Rh analog that contains 9-*cis*-retinal embedded in the same opsin environment.[2,3] Both are known to yield bathorhodopsin (bathoRh), a photoisomer that contains all-*trans*-retinal, via *cis–trans* isomerization of the 11 or 9 position upon absorption of a photon. Despite their similarity, the photoisomerization period and quantum yield is largely different. Rhodopsin photoisomerization is experimentally known to be faster ($t_{Rh} = 200$ fs,[4,5] $t_{isoRh} = 600$ fs[6]) and more efficient (quantum yield: $\Phi_{Rh} = 0.65$,[7] $\Phi_{isoRh} = 0.22$[8]).

Frutos et al. carried out a trajectory calculation on Rh.[9] Strambi et al. performed reaction path searches for Rh and isoRh.[10] They employed a dynamically correlated Quantum Mechanics (QM) method, but dynamics was treated for only one trajectory for Rh[9] and no dynamics calculation was done for isoRh.[10] In the latter paper, they described that molecular factors at the basis of the quantum yield difference remain to be understood.

In this study, we carried out Quantum Mechanics/Molecular Mechanics (QM/MM) trajectory surface hopping (TSH) direct dynamics calculations for Rh and isoRh with 162 runs for each in order to understand the origin of discrepancies in the rate and efficiency. Comparison is also made with our previous in vacuo calculations.[11,12] The transition probability is estimated using the Zhu–Nakamura (ZN) theory[13] of nonadiabatic transitions. The QM region is essentially a protonated Schiff base (PSB) of retinal (see Figure S1 in Supporting Information[22]). The rest of the molecules were treated with MM using mechanical embedding. The QM treatment was the 6-electron-6-orbital complete active space self-consistent field (CASSCF) technique[14,15] with the 6-31G basis set.[16] The MM part was described by AMBER parameters[17] in Gaussian 03.[18] Geometries of minima in the ground state and minimum energy conical intersections (MECI) are identified to analyze the dynamics results.

The excitation energy was overestimated by as much as 26 kcal mol^{-1} because we employed the CASSCF method. However, the errors would be tolerable for comparative study, and this will be seen later through the agreement of the dynamics results with experimental measurements.

We have already shown[11,12] that retinal molecule without opsin leads to rotations of ϕ_{11} and ϕ_9 in a direction opposite to each other. Thus, the essential feature of isomerization motion after photoexcitation is intrinsic in retinal itself.

The experimental photoisomerization period and bathoRh quantum yield were reproduced reasonably (Table 1). One of the slight differences between the simulation and experiments is due to the failure of the chosen QM/MM treatment to reproduce a ≈0.2 kcal mol^{-1} barrier[8,19] at the isoRh excited state reported in experiments. In our previous calculation,[11] we found a 10 kcal mol^{-1} barrier at the excited-state potential energy surface of an isoRh model system that caused trapping of trajectories. Even a tiny barrier in the present case would have slowed down the photoisomerization by trapping the trajectories in the excited state and yield a quantitatively accurate time scale and quantum yield.

Table 1 also shows that photoexcitation of Rh gives bathoRh (and the reactant) whereas the isoRh excitation yields a 9,11-di-*cis*-analog in addition to bathoRh (and the reactant). The 9,11-di-*cis*-rhodopsin (9,11-di-*cis*-Rh) has been characterized experimentally as a stable isomer of Rh and isoRh.[20] This by-product formation in isoRh photoisomerization would be another reason why life uses Rh rather than isoRh.

Shown in Figure 1 are the plots of the time evolution of the active dihedral angles (=C_{10}–C_{11}=C_{12}–C_{13}= or ϕ_{11} and =C_8–C_9=C_{10}–C_{11}= or ϕ_9, respectively) for the (a) Rh and (b) isoRh

Table 1. The ratio of photoproducts, quantum yield, and photoisomerization period of rhodopsin in comparison with isorhodopsin[a]

		Reactants	
		Rh(11-*cis*)	isoRh(9-*cis*)
Photoproducts/%	bathoRh(all-*trans*)	52 [27]	31 [13]
	isoRh(9-*cis*)	0 [22]	65 [82]
	Rh(11-*cis*)	48 [51]	0 [5]
	9,11-di-*cis*-Rh	0 [0]	4 [0]
Quantum yield	Calcd	0.52	0.31
	Exptl	0.65[7]	0.22[8]
Photoisomerization period/fs	Calcd	187 [185]	344 [665]
	Exptl	200[4,5]	600[6]

[a]The values in square brackets are taken from the corresponding gas-phase protonated Schiff base calculations.[11,12]

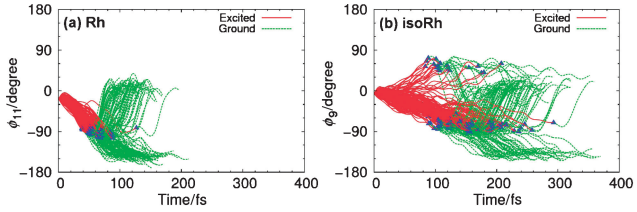

Figure 1. Time evolution of the dihedral angle of the twisting bond for the (a) Rh and (b) isoRh systems. Blue triangles are transition points from the excited state to the ground state.

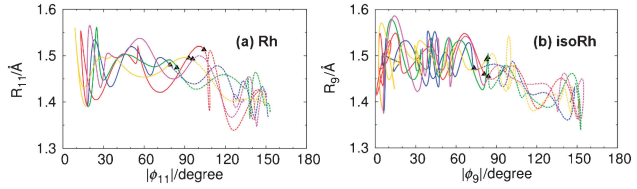

Figure 2. Change in length of the active bond $–C_n–C_{n+1}–$ against the absolute value of the dihedral angle $C_{n-1}–C_n–C_{n+1}–C_{n+2}$ for typical (a) Rh ($n = 11$) and (b) isoRh ($n = 9$) trajectories leading to the all-*trans*-form. The solid and dashed lines show that trajectories are in the excited and ground states and the black triangles correspond to transition from the excited state to the ground state.

trajectories. Clearly seen in Figure 1a is, for Rh, the lack of access of trajectories to a clockwise twist in ϕ_{11} in addition to rapid change in ϕ_{11} to $-90°$, where an MECI (minimum energy conical intersection) is located. Figure 1a shows that most of the trajectories are in a similar and simultaneous way in the excited state, consistent with vibrational coherence revealed in an experiment on Rh[21] although the present treatment of nuclei is classical except for transitions. In the case of isoRh (Figure 1b), a few trajectories are initiated by a clockwise twist of ϕ_9 in the excited state although the twist is unsuccessful and isoRh is regenerated in the ground state (S_0). Thus, all bathoRh photoproducts are formed via counterclockwise twist of the active dihedral ϕ_9 or ϕ_{11}. This obviously hindered isomerization is due to the constraints offered by the opsin environment especially by amino acid residues close to the binding pocket. In contrast, in our previous gas-phase PSB simulations, twists in both directions take place (cf. Figure 6, Ref 12). Also, it is revealed in Figure 1 that the twist is slower in isoRh than in Rh especially in the excited state.

Figure 2 shows the diagram of the active twist angle and the length of the active bond for five typical trajectories for Rh and isoRh. Fast and straightforward dynamics in Rh is shown in Figure 2a whereas complicated excited-state dynamics is evident in the isoRh case in Figure 2b.

Why is the isoRh photoisomerization more difficult than that of Rh? One reason is the atomic displacements required by the chromophore at the excited state potential energy surface to reach the conical intersection region. Shown in Figure 3 is a superimposed image of the S_0 optimized geometry and the geometry adapted by the chromophore at the crossing region. The pocket that contains the retinal chromophore is similar in shape for both the Rh and isoRh case. Opsin residues Thr118 and Tyr268 create a narrow gap near the $–C_9=C_{10}–C_{11}=$ region of the retinal chain with the two residues coming as close as 7 Å to each other. The isoRh photoisomerization is more difficult than that of Rh because of at least two reasons: (1) the isoRh isomerization requires more

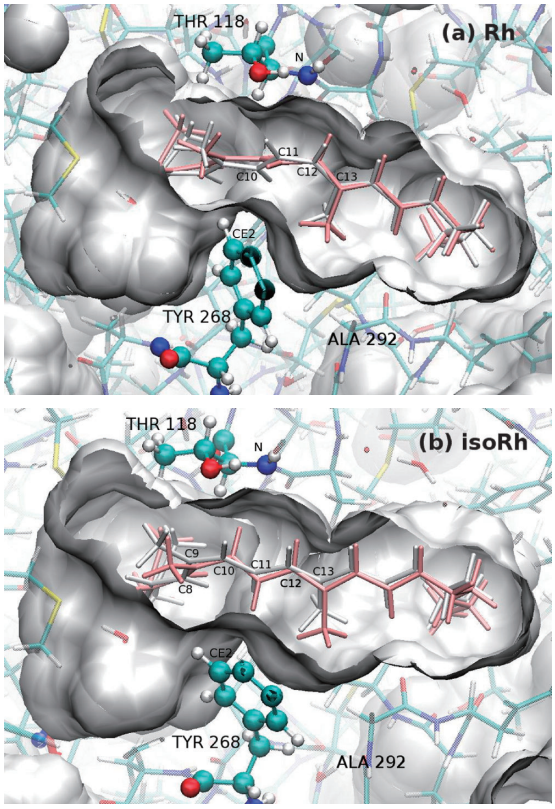

Figure 3. Superimposed structures of the S_0 optimized geometry (gray) and geometry at the MECI (pink) for the (a) Rh and (b) isoRh case. Also shown is the opsin pocket that contains the chromophore. The pocket surface is the overlapped envelope of amino residues surrounding the retinal chromophore, which is generated using the S_0 optimized geometry wherein the retinal chromophore is artificially removed.

Table 2. Initial interatomic forces between most relevant chromophore–opsin atom pairs[a]

	Force (hartree/bohr)	
	Rh	isoRh
Ret C_{12}-H-Cys187 O	$+2.5 \times 10^{-3}$	$+1.7 \times 10^{-4}$
Ret C_{10}-Tyr268 CE2[b]	$+2.2 \times 10^{-3}$	$+4.5 \times 10^{-4}$

[a]Positive signs show repulsive forces. [b]CE2: Tyr's second ε-carbon.

space than that of Rh and (2) the dihedral that needs to be twisted in the isoRh case ($–C_9=C_{10}–$) is situated within the narrow gap between Thr118 and Tyr268.

Another reason would be the initial acceleration of retinal atoms induced by surrounding residues. The initial force between two atoms for a few retinal–opsin atom pairs is listed in Table 2. Cys187 and Tyr268 are close enough to the chromophore to significantly influence the isomerization. For example, for the atomic distance between the C_{12} hydrogen in retinal and the oxygen in Cys187, the projected interatomic force for Rh is about 15 times larger than the counterpart for isoRh. Also, a fivefold difference is found for the force between retinal C_{10} and Tyr268. Such differences partially explain the discrepancy in the rate and efficiency of the *cis–trans* isomerization between the Rh and isoRh chromophores.

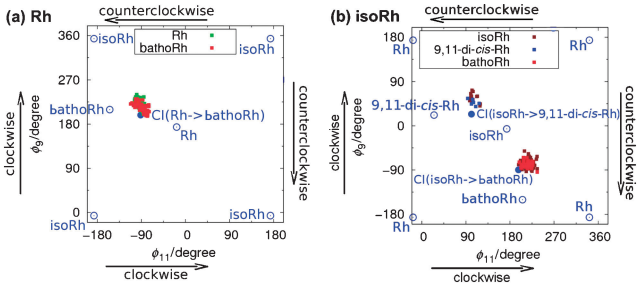

Figure 4. Diagram of the twist angles of $-C_{11}=C_{12}-$ (ϕ_{11}) and $-C_9=C_{10}-$ (ϕ_9) at the transition points. The minima in the ground state (open blue circles) and conical intersections (filled blue circles) obtained in the present calculations are plotted in the diagram. Rh: rhodopsin, isoRh: isorhodopsin, bathoRh: bathorhodopsin, 9,11-di-*cis*-Rh: 9,11-di-*cis*-rhodopsin, CI: minimum energy conical intersection.

Comparison with the previous gas-phase simulations reveals three other consequences shown below.

The protein causes (almost) one-way twisting of the active angle. As shown in Figure 4a, all of the Rh trajectories go through only one MECI region with clockwise-twisted ϕ_9 and counterclockwise-twisted ϕ_{11}. This MECI branches toward the formation of bathoRh (and the regeneration of the reactant). The relaxation of the excited state of isoRh, on the other hand, goes through two MECI regions, shown in Figure 4b. Most of trajectories from isoRh go through the MECI region with $\phi_9 \approx -90°$ and clockwise-twisted ϕ_{11}, which is shown as CI(isoRh → bathoRh). This MECI is responsible for all bathoRh generation. A few trajectories go through another MECI region (CI(isoRh → 9,11-di-*cis*-Rh)), which is responsible for 9,11-di-*cis*-Rh. Thus, photoexcitation of Rh only gives bathoRh as a product whereas isoRh yields 9,11-di-*cis*-Rh in addition to bathoRh, as shown in Table 1. Note that the reaction time is longer through CI(isoRh → bathoRh) ($\tau_{ave} = 233$ fs) than that through CI(isoRh → 9,11-di-*cis*-Rh) ($\tau_{ave} = 188$ fs). The difference is revealed in the dissimilarity in the twist speed of ϕ_9 in Figure 1b.

Second, the protein environment enhances the production of bathoRh. When the opsin environment was totally ignored, the calculated bathoRh (all-*trans*-PSB) quantum yield was only 0.27 and 0.13, respectively (in square brackets of Table 1). Explicit consideration of the opsin residues significantly improves the theoretical quantum yield to 0.51 and 0.31, respectively. This would be mainly due to the unidirectional rotation in opsin environment.

The third effect of the opsin on the dynamics is to cause transitions to take place near MECIs. Comparison of transition points in Figure 4 with those in Figure 11 in reference 11 and Figure 10 in reference 12 reveals that the present transition points with the opsin environment are nearer the MECI points than the points without the opsin. The opsin would prevent inefficient, premature hops especially in the isoRh case.

In conclusion, the faster and more efficient photoisomerization of Rh than of isoRh is due to a straightforward and fast excited-state dynamics for Rh in contrast with a complicated dynamics in a back-and-forth fashion especially in the excited state for isoRh. The dynamics is governed by the differences (1) in volume-saving motions of retinal molecules, (2) in space gaps formed by surrounding residues, and (3) in the initial acceleration by repulsive force from the surrounding amino residues. The formation of 9,11-di-*cis*-Rh by-product from isoRh photoisomerization is another reason why organisms adopt rhodopsin rather than isorhodopsin. The other effects of the opsin environment are (1) to cause the active dihedral angle in retinal to rotate one way, (2) to enhance the bathoRh quantum yield, and (3) to cause transitions to take place near the MECIs. The present scheme is found to be applicable to photoreactions of biomolecules.

Computations were partially performed at Research Center for Computational Science, Okazaki, Japan and Research Institute for Information Technology of Kyushu University. This research is supported by Grant-in-Aids for Scientific Research (C) No. 20608003 and (B) No. 19350013 from the Japan Society for the Promotion of Science (JSPS). WCC acknowledges the Kyoto University Start-Up Grant for Young Scientists.

References and Notes

1 F. Boll, *Am. J. Med. Sci.* **1878**, *151*, 190.
2 F. D. Collins, R. A. Morton, *Biochem. J.* **1950**, *47*, 18.
3 G. Wald, P. K. Brown, R. Hubbard, *Proc. Natl. Acad. Sci. U.S.A.* **1955**, *41*, 438.
4 R. W. Schoenlein, L. A. Peteanu, R. A. Mathies, C. V. Shank, *Science* **1991**, *254*, 412.
5 L. A. Peteanu, R. W. Schoenlein, Q. Wang, R. A. Mathies, C. V. Shank, *Proc. Natl. Acad. Sci. U.S.A.* **1993**, *90*, 11762.
6 R. W. Schoenlein, L. A. Peteanu, Q. Wang, R. A. Mathies, C. V. Shank, *J. Phys. Chem.* **1993**, *97*, 12087.
7 J. E. Kim, M. J. Tauber, R. A. Mathies, *Biochemistry* **2001**, *40*, 13774.
8 J. B. Hurley, T. G. Ebrey, B. Honig, M. Ottolenghi, *Nature* **1977**, *270*, 540.
9 L. M. Frutos, T. Andruniów, F. Santoro, N. Ferré, M. Olivucci, *Proc. Natl. Acad. Sci. U.S.A.* **2007**, *104*, 7764.
10 A. Strambi, P. B. Coto, L. M. Frutos, N. Ferré, M. Olivucci, *J. Am. Chem. Soc.* **2008**, *130*, 3382.
11 T. Ishida, S. Nanbu, H. Nakamura, *J. Phys. Chem. A* **2009**, *113*, 4356.
12 W. C. Chung, S. Nanbu, T. Ishida, *J. Phys. Chem. A* **2010**, *114*, 8190.
13 H. Nakamura, *Nonadiabatic Transition: Concepts, Basic Theories and Applications*, World Scientific Publishing Co. Pte. Ltd., Singapore, **2002**, p. 376.
14 H.-J. Werner, P. J. Knowles, *J. Chem. Phys.* **1985**, *82*, 5053.
15 P. J. Knowles, H.-J. Werner, *Chem. Phys. Lett.* **1985**, *115*, 259.
16 W. J. Hehre, R. Ditchfield, J. A. Pople, *J. Chem. Phys.* **1972**, *56*, 2257.
17 W. D. Cornell, P. Cieplak, C. I. Bayly, I. R. Gould, K. M. Merz, Jr., D. M. Ferguson, D. C. Spellmeyer, T. Fox, J. W. Caldwell, P. A. Kollman, *J. Am. Chem. Soc.* **1995**, *117*, 5179.
18 M. J. Frisch, G. W. Trucks, H. B. Schlegel, G. E. Scuseria, M. A. Robb, J. R. Cheeseman, J. A. Montgomery, Jr., T. Vreven, K. N. Kudin, J. C. Burant, J. M. Millam, S. S. Iyengar, J. Tomasi, V. Barone, B. Mennucci, M. Cossi, G. Scalmani, N. Rega, G. A. Petersson, H. Nakatsuji, M. Hada, M. Ehara, K. Toyota, R. Fukuda, J. Hasegawa, M. Ishida, T. Nakajima, Y. Honda, O. Kitao, H. Nakai, M. Klene, X. Li, J. E. Knox, H. P. Hratchian, J. B. Cross, V. Bakken, C. Adamo, J. Jaramillo, R. Gomperts, R. E. Stratmann, O. Yazyev, A. J. Austin, R. Cammi, C. Pomelli, J. W. Ochterski, P. Y. Ayala, K. Morokuma, G. A. Voth, P. Salvador, J. J. Dannenberg, V. G. Zakrzewski, S. Dapprich, A. D. Daniels, M. C. Strain, O. Farkas, D. K. Malick, A. D. Rabuck, K. Raghavachari, J. B. Foresman, J. V. Ortiz, Q. Cui, A. G. Baboul, S. Clifford, J. Cioslowski, B. B. Stefanov, G. Liu, A. Liashenko, P. Piskorz, I. Komaromi, R. L. Martin, D. J. Fox, T. Keith, M. A. Al-Laham, C. Y. Peng, A. Nanayakkara, M. Challacombe, P. M. W. Gill, B. Johnson, W. Chen, M. W. Wong, C. Gonzalez, J. A. Pople, *Gaussian 03 (Revision D.01)*, Gaussian, Inc., Wallingford CT, **2004**.
19 R. R. Birge, C. M. Einterz, H. M. Knapp, L. P. Murray, *Biophys. J.* **1988**, *53*, 367.
20 A. Trehan, R. S. H. Liu, Y. Shichida, Y. Imamoto, K. Nakamura, T. Yoshizawa, *Bioorg. Chem.* **1990**, *18*, 30.
21 R. M. Weiss, A. Warshel, *J. Am. Chem. Soc.* **1979**, *101*, 6131.
22 Supporting Information is available electronically on the CSJ-Journal Web site, http://www.csj.jp/journals/chem-lett/index.html.

